International Journal of Power and Energy Systems, Vol. 46, No. 10, 2026
An Open Access Paper

SVM OPTIMIZATION ALGORITHM FOR AUTOMATIC SEARCHING OF TRANSMISSION SECTION LIMIT BASED ON MULTI DEVICES STATE AWARENESS

Ye Zhang,* Qianpeng Hao,* Qi Guo,** Shun Yao,* Yifan Zhang,* and Qiang Li*

Abstract

Considering the variability of dynamic factors such as load fluctuations and power generation output in the power system, and the increased complexity of searching for transmission line limits. This study proposes a support vector machine (SVM) optimization algorithm based on multi device state perception technology for automatic search of the maximum power of transmission sections in power systems. Firstly, the topology structure of the power system is constructed using graph theory methods. Multiple device state data are collected through PMU devices, and the power composition matrix of the transmission line is solved using power flow tracking method as the input sample for SVM. The Whale Optimization Algorithm (WOA) is used to optimize the SVM parameters. To evaluate the transmission line power data based on the transmission line limit type, and achieve automatic search for transmission line limits. The experimental results show that the algorithm has a minimum search error of 0.1% in the IEEE 14 node system, and can accurately identify the maximum power of the section without manual review, achieving precise early warning of abnormal periods in temporary power trading scenarios.

Key Words

Multiple devices; State awareness; Transmission section limit; Automatic search; SVM optimization algorithm; Whale optimization algorithm

* Inner Mongolia Power (Group) Co. Ltd Inner Mongolia Power Electric Operations Control Company, Hohhot, 010010, China; e-mail: guyanye7ah@163.com, pohaoyaosmr@163.com, shunqiaofuh0@163.com, shuntengfan69@163.com, liaoshi76543@163.com Corresponding author: Qianpeng Hao
** Inner Mongolia Electric Power (Group) Co., Ltd. Hohhot Power Supply Company, Hohhot, 010010, China: e-mail: qiou08859063058@163.com

(DOI: 10.2316/J.2026.203-0623)

1. Introduction

The transmission section limit refers to the maximum active power that can be transmitted in the transmission section under the thermal stability constraints of all lines in the transmission section [1], which is an important index for measuring the transmission capacity of the transmission section. In an actual grid operation, the transmission cross-section is composed of a group of interrelated transmission lines (which may also include other components, such as transformers or generators). These lines operate the system to undertake the task of transmitting electric energy [2]. The determination of the transmission section limit is important to ensure the safe and stable operation of the power grid, which can help dispatchers better understand the transmission capacity of the power grid, so as to formulate a more reasonable scheduling plan to avoid the occurrence of overload or instability of the power grid [3]. In addition, the calculation of the transmission section limit is affected by many factors such as the grid structure, line parameters, and load level [4]. Therefore, in practical applications, it is necessary to analyze and calculate in detail according to the specific conditions of the power grid to ensure the accuracy and reliability of the results [5]. In summary, the transmission section limit is an important parameter for a safe and stable operation of the power system, which is of great significance for guaranteeing the transmission capacity and stability of the power grid.

The traditional transmission section limit analysis is obtained by power grid operation experts through offline analysis and manual selection. However, owing to the limitations of manual calculation and the increasingly complex power grid operation mode, it not only wastes a lot of time, but also cannot meet the needs of large-scale actual power systems [6]. At present, there is little research on the identification and automatic search methods of transmission sections, but there are many mature research results after consulting the research on transmission line state detection, including Bhattar et al.'s AC-DC multiphase power

flow algorithm for active distribution system analysis, the AC-DC multi-phase power flow algorithm can more accurately simulate the AC and DC power flow in the distribution system, especially in active power distribution systems containing complex equipment such as multi port power electronic transformers (PET). It can handle different voltage levels and different types of loads, including the flow of active and reactive powers. This enables the algorithm to consider various factors of the system more comprehensively and improves the accuracy and reliability of the transmission section limit assessment [7]. However, the accuracy of the AC-DC multiphase power-flow algorithm depends on largely on the accuracy of the model. If the model cannot accurately reflect the actual situation of the power system, such as the line parameters and load characteristics, then the calculation results of the algorithm may have deviations.

Patel studies the classification and location method of transmission line faults based on Lissajous superimposed component feature extraction. This method uses a Lissajous figure (the synthetic track of two sinusoidal vibrations in mutually perpendicular directions) to extract the superimposed quantitative features of the transmission line voltage and current signals, thus realizing the classification and location of the transmission line faults [8]. This method has a certain application prospect in the fault classification and location of transmission lines. However, there are still some challenges and limitations in the limit search of transmission sections. The performance of this method largely depends on the settings of the algorithm parameters, such as the fault detection threshold and sampling points. These parameter settings must be adjusted and optimized according to the actual situation, thereby increasing the difficulty and complexity of the algorithm application.

Shweta et al. studied the determination method of available transmission capacity (ATC) in competitive power markets, considered the uncertainty and randomness in power system operation, such as load fluctuations, new energy output changes, etc., and calculated the available transfer capability (ATC) through probability statistical methods. This method can more comprehensively reflect the actual situation of the power system and improve the accuracy and reliability of ATC assessments [9]. In a competitive power market, the uncertainty and randomness of power system operations increase significantly. These uncertainties include load fluctuations, new energy output changes, and equipment failure. How to effectively deal with these uncertainties and improve the accuracy and reliability of ATC assessments is an important challenge.

Sharma et al. studied a power cycle diagram and aggregation flexibility curve analysis method for active distribution networks to analyze power changes in active distribution networks. In active distribution networks, access to distributed power sources (such as solar energy and wind energy) will change the traditional power flow mode and generate new power cycles. By drawing the power cycle diagram, the size and direction of these cycle powers can be displayed intuitively, and their impact on the distribution network can be analyzed. The aggregated flexibility curve helps evaluate the flexibility and reliability of the distribution network and provides a basis for formulating reasonable dispatching strategies and planning schemes [10]. However, an active distribution network is a complex nonlinear system, and its operation mode and state are affected by many factors. It is difficult to accurately reflect the actual situation when building models of power cycle diagram and aggregation flexibility curve. For example, it may be difficult to accurately describe the output characteristics of distributed generation, load fluctuation rules, etc., which will lead to limited model accuracy and affect the accuracy of results.

Therefore, this article focuses on the problem of limit search in transmission intervals and studies the SVM optimization algorithm for automatic transmission interval limit search based on multi device state perception. In contrast, this paper innovatively constructs a comprehensive automatic search system for transmission section limits, encompassing "multi-device state sensing, power matrix modeling, and intelligent optimization classification." Through graph theory topological modeling, it achieves a precise abstraction of the connection relationships between power grid devices. By leveraging PMU devices to synchronously collect multi-dimensional state data such as voltage amplitude, phase angle, and power at a high sampling rate of 30 times per second, and combining it with power flow tracking methods to construct a generator-load power transmission quantification matrix, the system addresses the efficiency issues associated with traditional methods that rely on manual analysis. Innovatively combining the whale optimization algorithm with SVM, the system optimizes penalty factors and kernel function parameters to reduce extreme search errors to as low as 0.1%, significantly improving accuracy compared to a single SVM model. Additionally, for high-dimensional stable domain projection problems, t-SNE manifold learning is used for dimensionality reduction, with projection error controlled within 2%. The SMOTE algorithm and adaptive weighting mechanism are employed to address sample imbalance issues. Ultimately, this enables precise early warning of abnormal periods in scenarios such as temporary power transactions without manual review, achieving significant breakthroughs in dynamic adaptability, quantification accuracy, and engineering practicality compared to existing methods.

The main work of this paper focuses on the following research related to the automatic search for transmission section limits:

(1) Establish a multi-device state sensing system based on PMU to achieve synchronous collection of state quantities such as voltage, current, and power, and clarify the sampling frequency standard of 30 times per second and the GPS time synchronization mechanism.
(2) Propose a method for solving the line power composition matrix based on the power flow tracking method, and establish a generator-load power transmission quantification model.
(3) Designing a WOA-SVM optimization algorithm frame-

work, using the whale optimization algorithm to optimize the penalty factor and kernel function parameters of the SVM, thereby improving the classification accuracy of extreme states.

(4) Validating the algorithm's performance in the IEEE 14-node system, conducting experimental verification from four dimensions: steady-state accuracy, dynamic response, parameter optimization, and extreme state search.

2. SVM Optimization Algorithm for Automatic Searching of Transmission Section Limit Based on Multi-equipment State Perception

2.1 Transmission Section Limit State Analysis

The stability domain in the full-dimensional injection state space of a power system is a hyperplane that is difficult to describe directly, and downscaling is an inevitable choice. At present, the common method is to project it to the transmission cross-section of the stability domain described by the low-dimensional space, to the transmission cross-section power changes, on behalf of the full-dimensional injection space injection changes, the difference between the two leads to the stability domain boundary point is no longer uniquely determined, and become an "uncertainty interval" that is, the transmission cross-section power of the "limit interval", shown in Figure 1.

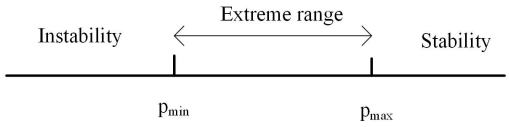

Figure 1. Limit State of Transmission Section

When the transmission cross-section power is less than the lower limit interval limit in Fig. 1, the base state and under the predicted faults remain safe and stable [11]. When the transmission cross-section power is greater than the upper limit of the limit interval, the base state or under the predicted faults will be the loss of safety and stability. The transmission cross-section power is greater than the lower limit of the p_{min} and less than the upper limit p_{max}, whether it is safe and stable is closely related to the actual operation arrangement. The rapid change in the output power of new energy plants and stations can lead to the expansion of the above limit range, and it is necessary to accurately identify the limit range and realize the cross-sectional limit search to help operators to grasp the security and stability boundaries of the power system operation and power market transactions [12].

To achieve an effective projection of high-dimensional stable domains onto the low-dimensional transmission section feature space, this paper employs the t-SNE manifold learning method for dimensionality reduction. This method preserves the local feature relationships in high-dimensional data, mapping the high-dimensional stable domain space to the low-dimensional transmission section feature space. It effectively captures the nonlinear associations between different equipment states and section limits, making it more suitable for the dimensionality reduction requirements of high-dimensional state spaces in power systems compared to PCA. Through this dimension reduction method, the stability domain of the full-dimensional injection state space, which is difficult to describe directly, can be transformed into quantifiable and analyzable low-dimensional transmission section limit intervals, laying the foundation for subsequent limit state identification.

2.2 Topological Representation of Power Systems Based on Graph Theory

In this paper, a graph is an abstract network consisting of "nodes" and "edges", which can be expressed $\psi = (\Omega, \vartheta)$, of which, ψ represents the power system topology diagram, Ω denotes the set of nodes (devices) in the power system topology graph, ϑ represents the set of edges (transmission lines) in a graph. If the direction of the edges is taken into account, the graph is classified as directed; otherwise, it is considered undirected. In cases where the edges in a directed graph are assigned a specific value, the graph is termed a weighted directed graph.

When disregarding the characteristics of the power system network components and considering only the active current of the system, the power system can be abstracted as a weighted directed graph. In this representation, the nodes correspond to the equipment within the system, the edges represent the system's lines, the weights of the edges denote the reactance values of the lines, and the direction of the edges indicates the flow direction of the current. Figure 2 illustrates a simplified power system topology.

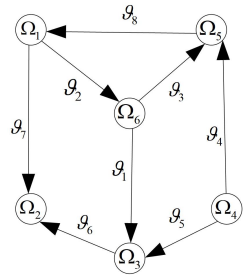

Figure 2. Topology Diagram of Power System

2.3 PMU Based Multi Device Status Awareness Data Acquisition Method

In the automatic search process of the transmission section limit of the power system topology map ψ, the PMU (phasor measurement unit) can synchronously measure the information [13] such as the voltage amplitude, phase angle, and branch power flow of each equipment node in ψ with a high sampling rate (typically 30times/s or higher). The power information encompasses active power and reactive power. These data provide the necessary input information for the automatic search of transmission section

limits, which facilitates accurate assessment of the transmission capacity and stability of the transmission section [14].

The PMU device continuously monitors and measures the power angles of multiple equipment online, as well as the amplitude and phase angle of voltage and current of each bus [15]. PMU devices are installed in each generator and hub substation in the power system and connected to the control center through the communication network. Each PMU collects the power angle simultaneously through GPS timing, and "sticks" the time scale to the measured power angle for real-time transmission to the control center [16]. The quantitative dimensions of equipment status sensing include: voltage amplitude (accuracy $\pm$ 0.5V), voltage phase angle (accuracy $\pm$ 0.01°), line active power (accuracy $\pm$ 0.5MW), reactive power (accuracy $\pm$ 0.3Mvar), and system frequency (accuracy $\pm$ 0.001Hz). Different PMU devices use a GPS second pulse synchronization mechanism, with time synchronization errors controlled within 1 μs. For sampling frequency differences ranging from 30 to 120 times per second, linear interpolation is used to resample the data, standardizing it to a 30 times per second sequence to ensure the temporal alignment accuracy of the state quantities. Figure 3 illustrates the schematic diagram of multi-device status sensing data acquisition, and Figure 4 presents the hardware structure block diagram of the PMU phasor measurement device.

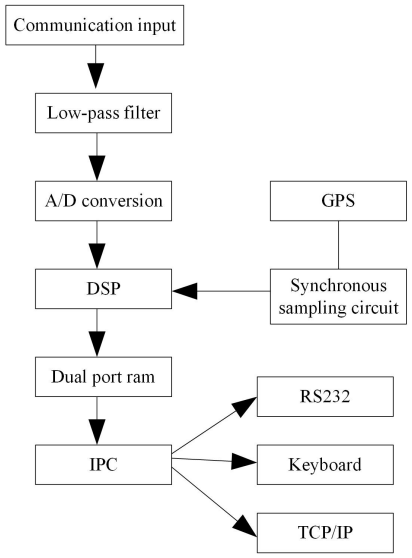

Figure 3. Multi Device State Aware Data Collection

The hardware structure of the PMU phasor measurement device primarily comprises analog input, synchronous sampling control, A/D conversion, microprocessor, IPC, and interface. The analog input part features multiple channels, enabling simultaneous measurement of voltage and current across multiple devices [17]. Voltage or current signals from the secondary side, following isolation transformation and analog low-pass filtering, are received by the synchronous sampling system established on the GPS time reference. These signals are sequentially converted by A/D and put into the fixed RAM. Utilizing

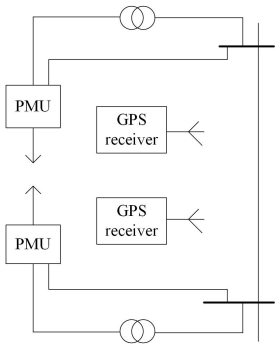

Figure 4. Schematic Diagram of Synchronous Phasor Measurement

the discrete Fourier transform algorithm, the DSP calculates the fundamental wave components of all measured phases and their corresponding positive sequence components once every sampling period. Subsequently, it incorporates the time information provided by the GPS receiver serial port and the sequence number of the first sampling point in the data window to generate calculation results, appending a readily identifiable time tag [18]. The industrial computer performs additional calculations and displays each synchronization vector. The calculated results, along with their time tags, are transmitted to the data server in the monitoring center through the RS232 serial port or Ethernet interface, in accordance with the communication protocol requirements for subsequent transmission section limit search.

PMU deployment follows the N-1 safety principle, with 100% coverage of critical generator nodes, $\leq$ 90% coverage of 220kV and above hub substations, and $\leq$ 85% coverage of important load centers. For unmonitored nodes, a state estimation algorithm based on weighted least squares is used to perform interpolation calculations using measurement data from adjacent monitored nodes, with an estimation error of $\leq$ 2%, meeting the accuracy requirements for limit analysis.

2.4 Line Power Composition Matrix Solving Based on the Current Tracking Method

In the automatic transmission section limit search, it is necessary to use the current tracking algorithm, combined with the multi-device state awareness measurement data obtained in Subsection 2.3, to simulate and analyze the distribution of the current in the line, and then analyze whether there is a section limit power in the transmission line. Based on the multi-device state-aware measurement data acquired in Subsection 2.3, the line power matrix can be constructed by utilizing the current tracking algorithm and the principle of proportional distribution. One of the basic principles of trend tracking is proportional allocation, which observes the change in the trend of the transmission section by continuously adjusting the generation equipment and load in the grid [19], [20].

In the power grid, the node output line current is formed by the node of the input line current combination the line

due to resistance and reactance losses, moved to both ends of the line as an equivalent load. The grid can be viewed as a lossless network [21]. At this point, we can obtain the node output line power composition ratio and node input line power, considering that the proportion of the node's total injected power is the same. The proportional distribution principle is shown in Figure 5.

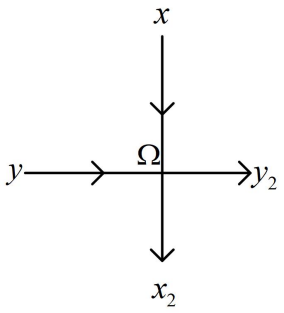

Figure 5. Schematic Diagram of Proportional Distribution Principle

The arrows in Fig. 5 indicate the direction of flow of the line power, and it can be seen that for the node Ω, the total inflow and outflow powers are equal. Set the power flow through the node Ω on the transmission line x to the line y, according to the principle of proportional distribution:

$$p_{xy} = 10 \times \frac{20}{20+40} = \frac{10}{3} \tag{1}$$

The power system is abstracted as a directed graph, where the weights of the edges are reactance values of the lines. Assuming that the number of generators in the power system is M_η, the number of loads is M_λ, the number of bypasses is M_ϑ, establish the node-branch correlation matrix to obtain the matrix Γ_ϑ of generator contribution factors to line currents, and the matrix Γ_λ of load draw factors on line currents, based on the matrix Γ_ϑ and Γ_λ, the power composition matrix of all lines in the system can be obtained.

The power composition matrix p of M_ϑ branches is represented by Equation (2).

$$p = \begin{bmatrix} p_{1-1-1} & \cdots & p_{1-1-M_\lambda} & p_{2-1-1} & \cdots & p_{2-1-M_\lambda} & \cdots & p_{M_\eta-1-1} & \cdots & p_{M_\eta-1-M_\lambda} \\ p_{1-2-1} & \cdots & p_{1-2-M_\lambda} & p_{2-2-1} & \cdots & p_{2-2-M_\lambda} & \cdots & p_{M_\eta-2-1} & \cdots & p_{M_\eta-2-M_\lambda} \\ \vdots & \ddots & \vdots & \vdots & \ddots & \vdots & \ddots & \vdots & \ddots & \vdots \\ p_{1-M_\vartheta-1} & \cdots & p_{1-M_\vartheta-M_\lambda} & p_{2-M_\vartheta-1} & \cdots & p_{2-M_\vartheta-M_\lambda} & \cdots & p_{M_\eta-M_\vartheta-1} & \cdots & p_{M_\eta-M_\vartheta-M_\lambda} \end{bmatrix} \tag{2}$$

Set the element $p_{\eta-\theta-1}$ represents the active power transmitted by the generator η via the line ϑ to the load λ. The defined power composition matrix of the line is a key quantitative model derived based on the power flow tracing method, and its construction process follows the principles of power conservation and proportional allocation in the power system. This matrix clearly presents the distribution relationship of active power transmitted from different generators to loads through various lines by integrating the generator contribution factor matrix and the load extraction factor matrix. The significance of this formula lies in transforming the complex power flow relationship of the power grid into a structured matrix form, providing intuitive and comprehensive input features for subsequent SVM models, enabling the model to judge the load state of the transmission section based on specific power allocation data. It is an important bridge connecting multi-device state perception data and limiting search results, ensuring a refined analysis of the power composition of the transmission section.

2.5 Automatic Searching Algorithm of Transmission Section Limit Based on SVM Optimization

Utilizing the line power matrix p constructed in subsection 2.4 as the input sample of the SVM model, the SVM model determines whether the line power is in the section limit state based on the recognition result of the power value state, thereby facilitating the automatic search of the section limit. This process can be completed without manual analysis. The complete execution process of the algorithm from power grid topology modeling to extreme state warning, covering the entire process of data collection, processing, modeling, and optimization decision-making, is shown in Figure 6.

2.5.1 Automatic Searching of Transmission Section Limit Based on SVM

Support Vector Machine (SVM) has been extensively used in power system. SVM is a machine learning algorithm founded on statistical learning theory. It effectively mitigates the "dimension disaster" and "over learning" challenges, demonstrating robust generalization capabilities. SVM is particularly suitable for addressing the rule extraction problem in samples characterized by volatility, intermittency, and high dimensionality. The fundamental principle of SVM involves categorizing line power matrix data sets by identifying the optimal division plane (or hyperplane) [22].

Given the n dimensional transmission line power sample set as training samples $p_n = (p_j, \varphi_j)$, p_j as input the transmission line power vector under multi-device state awareness; φ_j is the output vector, which represents the target attribute set and the identification result of the limit state of the transmission section, that is, the result of the automatic limit search.

The nonlinear regression decision function for the au-

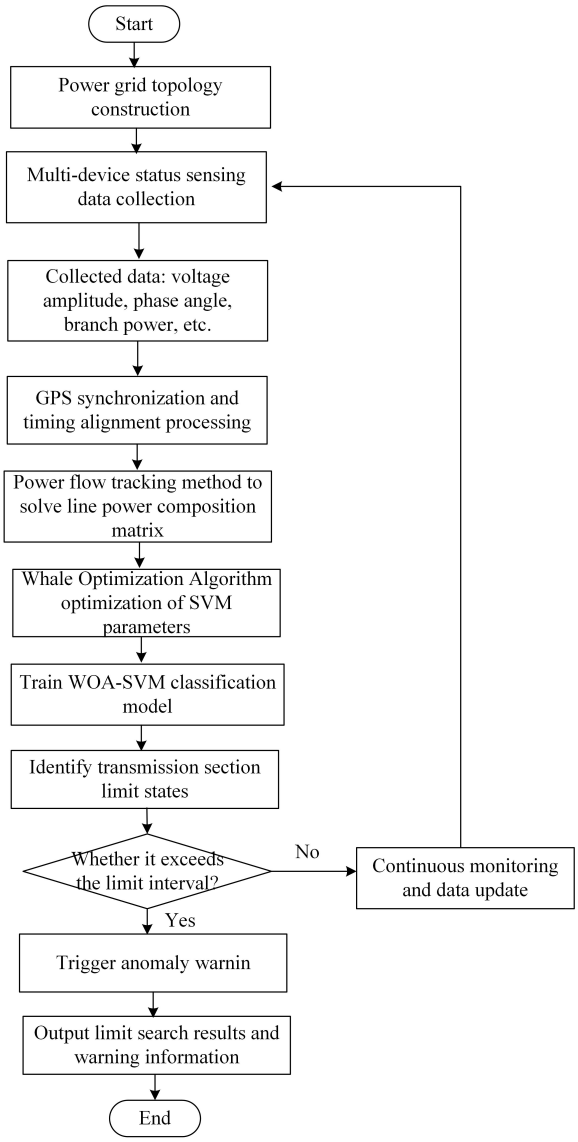

Figure 6. Flow Chart of SVM Optimization Algorithm for Automatic Search of Transmission Section Limit Under Multi-device State Perception

tomatic search of the transmission section limits is given by:

$$f(p,\varphi)=\sum_{j=1}^{n}\left(\beta_j^*-\beta_j\right)K(p_i,p_j)+c \tag{3}$$

In the formula, $K(p_i,p_j)$ is the kernel function, which maps the input line power matrix vector space, to a high-dimensional eigenvector space. β_j^*, β_j are Lagrange multiplier. c is the offset. This function maps the input low dimensional line power matrix data to a high-dimensional feature space by introducing a kernel function, thereby constructing a linear classification hyperplane in the high-dimensional space and solving the problem of difficult linear partitioning of transmission section limit states in the low dimensional space. The physical significance lies in transforming complex power state data of transmission sections into quantifiable classification results, capturing the implicit correlation between power data and limit states through the nonlinear mapping ability of kernel functions, providing a mathematical basis for automatic identification of transmission section limits, and enabling accurate judgment of whether the line power is in the limit range in scenarios with dynamic changes of multiple devices.

Introducing slack variables α, of which α is the upper limit of the slack variable,α is the lower limit of the relaxation variable, and the specific optimization function is:

$$\begin{cases} \min g(\mu)=\frac{1}{2}\|\mu\|^2+B\sum_{j=1}^{n}(\alpha_j+\bar{\alpha}_j) \\ \text{s.t. } \varphi_j-K(\mu,p)-c\le\partial+\alpha_j \\ K(\mu,p)+c-\varphi_j\le\partial+\bar{\alpha}_j \\ \alpha_j,\bar{\alpha}_j\ge 0 \end{cases} \tag{4}$$

In the formula, ∂ is the fitting accuracy of the results of the automated search for transmission cross-section limits; B is the penalization factor; $K(\mu,p)$ is the kernel function. The penalty factor is a manually set parameter used to penalize the misidentified training samples. It regulates the balance between the interval and accuracy. The larger the value, the less the model is willing to give up those outliers, that is, the more important it attaches to the accuracy of the recognition results of automatic transmission cross-section limit search; the smaller the value, the less the model attaches importance to those outliers, that is, it pays more attention to the size of the interval.

This label was generated using PSCAD/EMTDC offline simulation, covering four scenarios: normal state (50%), lower limit range (20%), upper limit range (20%), and out-of-limit state (10%). It encompasses 200 typical fault conditions and 100 load fluctuation scenarios. To address the issue of sample imbalance, the SMOTE algorithm was used to oversample the minority class samples (out-of-limit state). Additionally, an adaptive weighted SVM mechanism was employed to assign a 1.5-fold weighting coefficient to out-of-limit samples, thereby enhancing the model's sensitivity in identifying extreme states.

The study found that the penalization factor and Band parameters in the kernel function play a very important role in the performance of the SVM algorithm. They primarily determine the accuracy and generalization ability of the SVM. If the random parameter selection method is adopted, the maximum precision and generalization ability of the model training are often not achieved, so a parameter optimization method is needed.

2.5.2 SVM Parameter Optimization Training Based on Whale Optimization Algorithm

The WOA is a relatively new metaheuristic swarm intelligence optimization algorithm proposed by Mirjalili and Lewis in 2016, which mimics the "spiral bubble net" predatory strategy of humpback whales. In the whale optimization algorithm [23], the whale population can be represented by a set of vectors, and each vector represents the position of a whale. These positions correspond to the parameter combination of the SVM in the algorithm.

The WOA algorithm optimization steps are as follows:

(1) Circling the prey

Humpback whales can identify and circle the location of their prey. Taking the current optimal whale position (the optimal solution of the current SVM parameter combination) as the optimal search agent, the mathematical expression of the position update is:

$$A = |DZ^*(t) - Z(t)| \tag{5}$$

$$Z(t+1) = Z^*(t) - EF \tag{6}$$

In the formula, t is the number of iterations, and is the number of optimization of SVM parameter combination; E and D are the coefficients. $Z^*(t)$ is the best whale position vector obtained at present, which will be updated with the size of fitness in each iteration. The fitness value is set as the error rate of the transmission line power data identification in the automatic search result of the SVM pair representing the transmission section limit, hereinafter referred to as the error rate of the limit automatic search; $Z(t)$ is the current whale position vector that represents the combined solution of the current SVM parameters; F is the iterative distance for the current whale position to approximate the current best whale position. The updated formula for E and D are:

$$E = 2os_1 - o \tag{7}$$

$$D = 2s_2 \tag{8}$$

In the formula, o is a random parameter that decreases linearly from 2 to 0 during the search iterations. s_1 and s_2 are random numbers with in $0 \sim 1$.

(2) Spiral trapping
Humpback whales swam in a contracting circle while following a spiral path toward prey, modeling this simultaneous behavior. It is assumed that there is a 50% probability that a choice can be made between the constricted circle or spiral model to update the position of the whale. This process is mathematically modeled as:

$$Z(t+1) = \begin{cases} Z^*(t) - EF & w < 0.5 \\ F'cos(2\pi v) + Z^*(t) & w \geq 0.5 \end{cases} \tag{9}$$

In the formula, w is a random number of [0,1]. F' is the distance between each whale and current optimal whale position. In this study, it represents the difference between the current iterative solution of the SVM parameter combination and the optimal solution; v is a random number of [-1,1].

$$F' = |Z^*(t) - Z(t)| \tag{10}$$

When attacking prey, mathematically set close to the prey, theowill decrease. From Eq. (7), with the o decreases linearly, E fluctuates within $[-o, o]$ range; when E is in the range [-1,1], the next position of the whale can be any position between its present position and the prey position, and the algorithm sets that the $E < 1$, when the whale attacks the prey, it approaches the prey position according to Equation (10).

(3) Searching for prey
When searching for prey, based on E to determine whether to select SVM parameter combination to solve the random search mechanism. When $E \geq 1$, the search model used are:

$$F = |DZ_r(t) - Z(t)| \tag{11}$$

$$Z(t+1) = Z_r(t) - EF \tag{12}$$

In the formula, $Z_r(t)$ is the randomly selected whale position vector, and is the randomly selected SVM parameter combination solution. When $E \geq 1$, a search agent is randomly selected to update the position of other whales with the randomly selected whale position vector, force the whales to deviate from their prey, and search for more suitable prey, thereby enhancing the global search ability of the algorithm to optimize the combination of SVM parameters.
The final obtained whale position vector Z^* is the optimized combination of SVM parameters. In this paper, WOA algorithm is used to optimize the setting of learning parameter penalty coefficient and sum parameter in SVM.

In summary, the optimization steps of support vector machine parameters based on the whale optimization algorithm are as follows:

(1) Initialization
Establish the parameters for the whale optimization algorithm, including the determination of the number of whales (also referred to as population size, which represents the quantity of candidate solutions for SVM parameter combinations), the initial position of each whale (search initiation point), and the maximum number of iterations (the quantity of iterations required to identify the optimal solution for SVM parameter combinations within the search space).

(2) Adaptation assessment
For each whale individual (that is, a set of candidate solutions of SVM parameters), the SVM model is used to train the power data of the transmission line, and its limit automatic search error rate is evaluated. This performance will be used as the fitness value of the whale individual.

(3) Updating whale locations
In accordance with the search mechanism of whale optimization algorithm, the positions of whale individuals are updated, thereby updating the combined value of SVM parameters. During each iteration, the optimal solution within the current population (i.e. the whale individual with the minimum fitness value) and its corresponding SVM parameters are recorded.

(4) Obtaining the optimal parameters
In each iteration, the optimal solution in the current population (that is, the whale individual with the minimum error rate of the automatic search limit) and its corresponding SVM combination parameters are recorded. Finally, the automatic search the result of transmission section limit is output from equation (3),

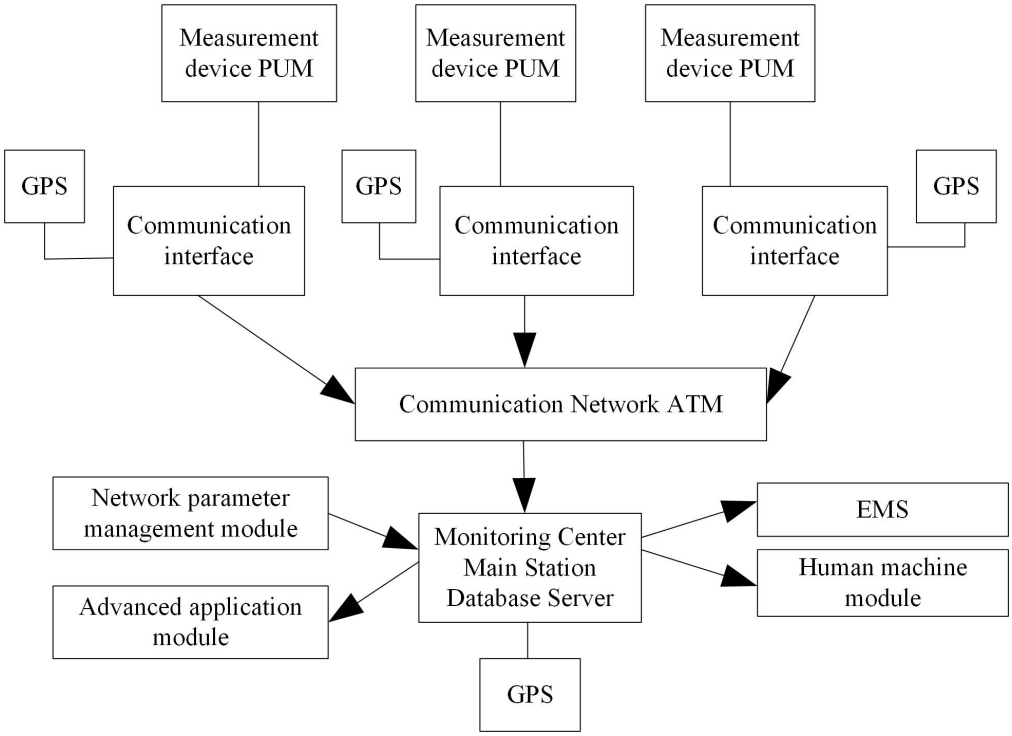

Figure 7. Structure of Power Grid Monitoring System Based on PMU

that is, whether the power of transmission line belongs to the automatic search the result of section limit power.

3. Experimental Analysis

3.1 Experimental Design

In the experiment, the algorithm is used in the power grid monitoring system based on the PMU to search for the transmission section limit. The system structure is shown in Figure 7.

As shown in Figure 7, the monitoring master station can accurately receive and forward the measurement data from the PMU, use different databases to realize the periodic storage of data, and exchange data with other systems. The IEEE14 bus system is selected to verify the proposed method, and Matpower is used for the power flow calculation. The key transmission section of the transmission section is automatically calculated according to the algorithm proposed in this study. Figure 8 shows the IEEE 14 node system architecture. The generator nodes in the IEEE 14 node system are Node 1 and Node 2, and the other nodes are load nodes.

The dataset covers multi-scenario operation data of IEEE 14 nodes, including continuous high-frequency monitoring data for 168 hours (7 days), with a total sample size of 172800 groups (30 times/second × 3600 seconds × 168 hours), covering 30 typical load fluctuation conditions, 25 new energy output fluctuation scenarios, and 15 equipment fault simulation states. The proportion of extreme state samples has increased to 20%.

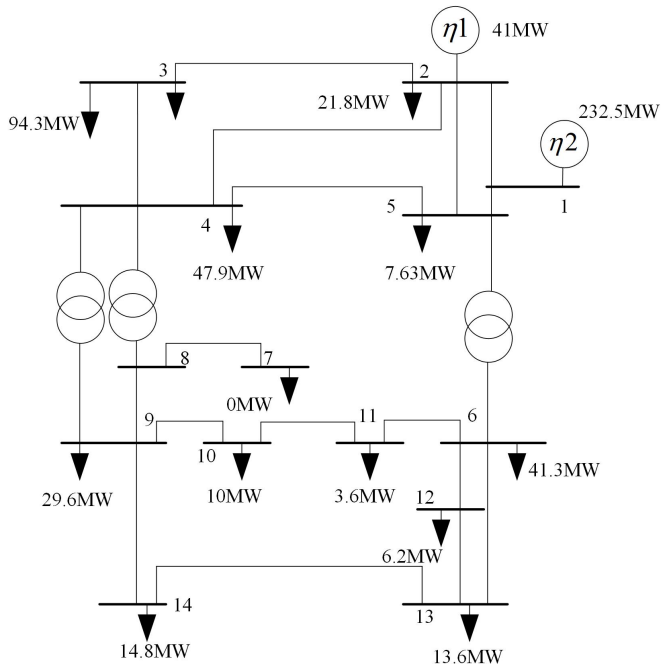

Figure 8. IEEE 14 Node System Architecture

3.2 Validation of the Effectiveness of Multi-devices State Awareness

3.2.1 Steady-state Output Performance Verification

When the PMU device used in this algorithm senses the status data of multiple devices, steady-state output performance is tested. The accuracy performance indicators of the AC voltage amplitude and frequency output of the

PMU device are tested using the three-phase AC power standard. The main technical indicators that the PMU device can reach: AC signal amplitude accuracy is not more than ± 0 5V; The frequency accuracy shall not be greater than ± 0.001 Hz. See Table 1 and Table 2 for the test results.

Table 1
Steady State Output Effect of Voltage Amplitude

Measurement line	Output Value /V	Actual measurement value /V
2-3	95	94.9
4-5	95	94.9
7-8	98	97.9
9-10	69	69
10-11	97	96.9
6-11	93	92.9
13-14	86	85.9

Table 2
Frequency Steady-state Output Effect

Measurement line	Output Value / Hz	Actual measurement value / Hz
2-3	46	46.001
4-5	51	51.001
7-8	56	56.001
9-10	58	58.001
10-11	61	61.001
6-11	63	63.001
13-14	70	70.001

As shown in Table 1 and Table 2, the measurement deviation values of the AC voltage amplitude and frequency output by the PMU device used in this algorithm are only -0.1V, +0.001 Hz. The performance of the PMU device is in line with expectations and can be used for multi device status perception.

3.2.2 Dynamic Output Performance Validation

For the dynamic output performance test when the PMU device senses the status data of multiple devices, use a high-speed signal acquisition analyzer to record and evaluate the output response process as the output amplitude of the PMU tester undergoes stepwise changes. Subsequently, employ the high-speed signal acquisition analyzer in conjunction with RecordPlayer analytic software to record the test results.

Add a sudden load signal to the three-phase voltage circuit in which the PMU device is located, and conduct testing with the primary voltage step state. The step transition waveform is shown in Figure 9.

As shown in Figure 9, when the load in the power system suddenly increases, the stability of the system may be affected if the power generation and transmission capacity of the system remain constant. In this case, the voltage may decrease owing to the sudden increase in load, because the generator needs to provide more power to meet the new

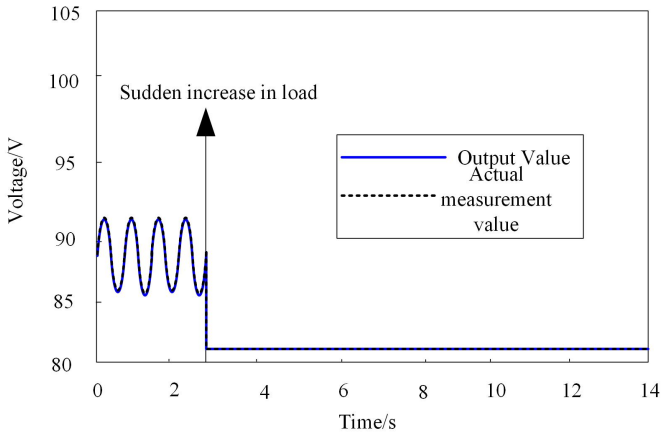

Figure 9. Dynamic Output Performance Detection Effect

load demand, which may lead to a voltage drop. In this algorithm, the deviation between the measurement results of the PMU and the actual results is very small, and the dynamic output performance test results are ideal.

3.3 Validation of the Effectiveness of Multi-devices State Awareness

Using the power flow tracking method described in Subsection 2.4, the active power flowing to the load point from generators $\eta 1$ and $\eta 2$ through the transmission line is calculated. The results are shown in Table 3.

Table 3
The Active Power of the Generator Flowing Through the Transmission Line to the Load Point

Line Coding	$\eta 1$	$\eta 2$
Route 1-2	2.63	0
Route 1-5	4.89	0
Route 2-3	0	0
Route 2-4	0	0
Route 2-5	2.2	0.54

Due to the limitation of space, only the power composition of some lines is shown in the paper. Taking node 5 as an example, the active power required by the load at this node is all provided by the generator $\eta 1$ and $\eta 2$, as can be seen from Figure 8, the generator $\eta 1$ and $\eta 2$ provide the active power to node 5, which eventually all flows through lines 1-5 and 2-5, it is obtained from Table 1 that the power provided by the generator $\eta 1$ for node 5 is 4.89MW + 2.2MW = 7.09MW, the power provided for node 5 by the generator $\eta 2$ is 0.54 MW, and the sum of the two is equal to the load of node 5 of 7.63 MW. Therefore, the power composition matrix of the line can accurately reflect the power flow results of the system line.

3.4 SVM Parameter Optimization Performance Verification

After training the SVM parameters using the whale optimization algorithm, the parameters are optimized. The

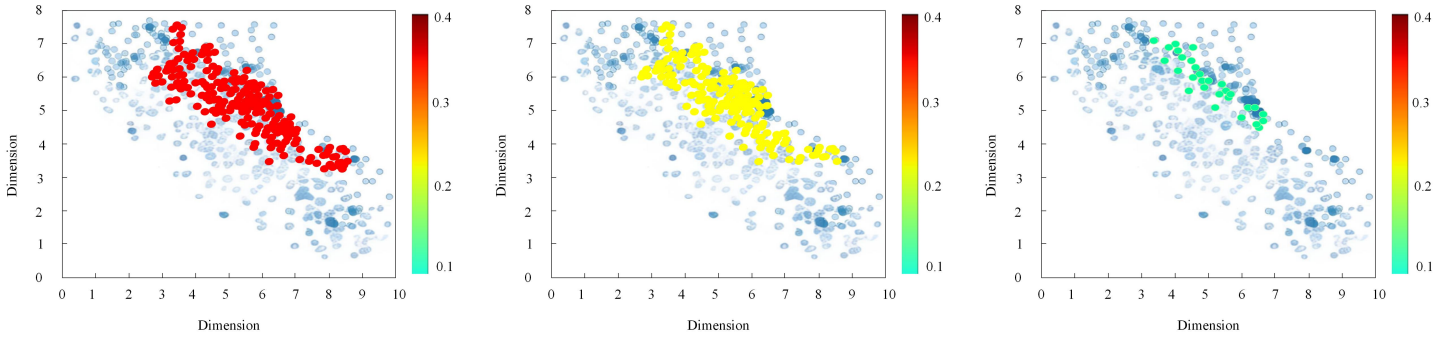

(a) Error Distribution Before Training SVM Parameters Using Whale Optimization Algorithm

(b) Error Distribution After 10 Iterations of Training SVM Parameters

(c) Error Distribution After 20 Iterations of Training SVM Parameters

Figure 10. Visualization of Error Distribution in the Iterative Process of Whale Optimization Algorithm Training SVM Parameters

target accuracy rate is set to 98%, and the maximum number of iterations is set to 20. To visualize the optimization process of the SVM parameters, the iteration process of training the SVM parameters using the whale optimization algorithm is shown in Figure 10. The blue dots in Figure 9 represent the distribution of labeled samples in the training set, and the unit of the error coefficient on the right is %.

Figure 10 (a) shows that before the algorithm in this study uses the whale optimization algorithm to train SVM parameters, Figure 9 (b) shows the error distribution after 10 iterations of training SVM parameters, and Figure 9 (c) shows the error distribution after 20 iterations of training SVM parameters, as shown in Figure 10, where the whale optimization algorithm is used to train the SVM parameters, and the error of the SVM's automatic search for transmission section limits can be further reduced to the minimum value of 0.1% after 20 iterations, and the test accuracy of the model is also improved.

3.5 Performance Validation of Automatic Transmission Section Limit Search

The comprehensive safety and stability limit power of the transmission section refers to the maximum power that can be transmitted by the transmission section under the condition of satisfying safe and stable operation of the power grid. Temporary power trading leads to sudden changes in the transmission power of the transmission section. When the power involved in a transaction is large, it may exceed the safety and stability limits of the transmission section. Set the transmission scenario as shown in Figure 11. The minimum and maximum limit power of the transmission section are 18 MW and 40 MW, respectively. Temporary power transactions occur between 8.9 h and 9.1 h, resulting in the limit power of the transmission section exceeding the maximum value of 40 MW. At this time, an effective algorithm is required to automatically search and mark the power segments that exceed the limit and send an early warning. In this scenario, the algorithm in this study automatically searches for the result tag, and the limit alarm alert results sent by the power grid monitoring system based on PMU are shown in Figure 11 and Table 4.

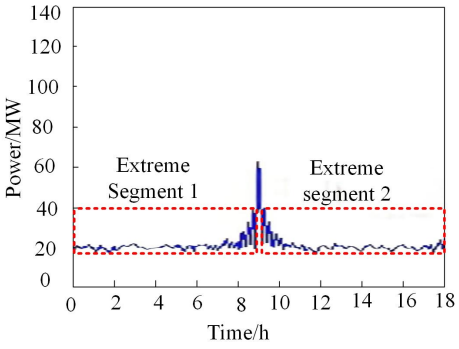

Figure 11. Automatic Search Conditions and Labeling Results for Transmission Section Limit

Table 4
Limit Alarm Reminder Results Issued by PMU-based Power Grid Monitoring System

Time/h	Alarm reminder content
8.1	No advance warning reminder
8.3	No advance warning reminder
8.5	No advance warning reminder
8.7	No advance warning reminder
8.9	Extreme power exceeding maximum warning
9.1	Extreme power exceeding maximum warning
9.3	No advance warning reminder
9.5	No advance warning reminder
9.7	No advance warning reminder
9.9	No advance warning reminder

As shown in Figure 11 and Table 4, under the condition of automatic search of transmission section limit, after the algorithm in this paper automatically searches the section limit power, the power in the marked limit section 1 and limit section 2 interval meets "the minimum and maximum limit power of transmission section are 18 MW and

Table 5
Verification Results for Different Grid Scales and Typical Regional Scenarios

Number of nodes	Scenario Type	Deviation rate of line parameters /%	Extreme search error /%	Recognition accuracy /%	Warning response time /ms
100	Conventional plain power grid	2	0.15	99.0	29.1
	High humidity coastal power grid	5	0.17	98.6	33.2
	High altitude inland power grid	8	0.19	98.4	35.5
200	Conventional plain power grid	0	0.17	98.8	29.7
	High humidity coastal power grid	5	0.19	98.4	33.8
	High altitude inland power grid	8	0.21	98.2	36.2
500	Conventional plain power grid	0	0.19	98.5	30.5
	High humidity coastal power grid	5	0.22	98.1	34.5
	High altitude inland power grid	8	0.24	97.9	37.0

40 MW respectively, and temporary power transaction occurs between 8.9h and 9.1h, resulting in the limit power of transmission section exceeding the maximum value of 40 MW" this actual situation, and after using the algorithm in this paper, the PMU based power grid monitoring system sends out the limit alarm reminder results show that 8.9h and 9.1h have extreme power exceeding the maximum warning, and there is no alarm reminder in other periods. This alarm reminder result is consistent with the objective reality, and this alarm reminder result is consistent with the actual situation. There is no need to manually review the data to send an early warning, which verifies the effectiveness and accuracy of this algorithm.

Select 100-node, 200-node, and 500-node systems, covering three typical regional scenarios: conventional plain power grids, high-humidity coastal power grids, and high-altitude inland power grids, to verify the adaptability and stability of the proposed algorithm in different power grid scales and complex geographical environments. The results are shown in Table 5.

Analyzing Table 5, as the number of grid nodes increases from 100 to 500, the maximum search error for conventional plain grids increases from 0.15% to 0.19%, the identification accuracy rate decreases from 99.0% to 98.5%, and the warning response time extends from 29.1ms to 30.5ms. This indicates that the expansion of grid scale has a minor impact on algorithm accuracy and efficiency, but overall performance remains at a high level. In typical regional scenarios, under the same node scale, the maximum search error of high-humidity coastal power grids (parameter deviation of 5%) increased by an average of 0.02-0.03% compared to conventional plain power grids, the recognition accuracy decreased by 0.4-0.5%, and the warning response time increased by 3.5-4.0 ms; In high-altitude inland power grids (parameter deviation of 8%), performance changes are more significant, with the maximum search error increasing by 0.04–0.05% compared to conventional scenarios, recognition accuracy decreasing by 0.6–0.8%, and warning response time increasing by 6.4–6.5 ms. This indicates that the higher the line parameter deviation rate, the greater the impact on algorithm performance. Despite these changes, the extreme search error in all scenarios is controlled within 0.24%, the recognition accuracy remains above 97.9%, and the warning response time does not exceed 37 ms, meeting engineering practical requirements. The proposed algorithm has been validated for its adaptability across different grid scales and typical regional scenarios. Even in environments with significant parameter deviations, such as high humidity and high altitude, it maintains high extreme search accuracy and fast response speeds, providing reliable technical support for the safe and stable operation of power grids in complex geographical environments.

By conducting a quantitative analysis of the projection errors of different dimension reduction methods, this study verifies the optimal dimension reduction scheme applicable to the extreme search scenario of transmission line cross-sections. It clarifies the performance differences between t-SNE manifold learning and PCA in terms of preserving high-dimensional data features and controlling projection errors, and evaluates the extent to which the dimension reduction process affects the width of the extreme interval of transmission line cross-sections. The results are shown in Table 6.

Table 6
Dimension Reduction Methods and Projection Error Analysis Results

Dimension reduction method	T-SNE manifold learning	PCA
KL divergence error	0.018	0.035
Average projection error /%	2.1	4.3
Maximum interval width increase /%	3.2	5.7
Adjusted interval error /%	0.8	2.3

Analyzing Table 6, when using the t-SNE manifold learning method for dimensionality reduction, the high-dimensional stable domain projection process can cause the width of the limit interval to increase by up to 3.2%. By introducing a correction factor (k=0.97) to compensate for the projection results, the error in the limit interval can be controlled within 1%, having a minimal impact on the accuracy of the limit search for transmission cross-sections. In contrast, the projection error of the PCA method has a

greater impact on the width of the limit interval, with an error of 2.3% remaining even after correction, thereby validating the applicability and superiority of t-SNE manifold learning in this study.

4. Conclusion

The research and analysis of the transmission section limits can provide a comprehensive understanding of power grid operational characteristics and potential risks, thereby ensuring the safe and stable operation of the power grid. Furthermore, the study of transmission sections is essential for online rapid security analysis of large power grids, which is crucial for enhancing the safe operation and accident prevention capabilities of power grids. This paper proposes an SVM optimization algorithm for automatic searching of transmission section limit based on multi-equipment state perception. After optimizing the SVM parameters through WOA, the automatic search error for the transmission section limit can be reduced to 0.1%. In different scale power grids such as 100 nodes, 200 nodes, and 500 nodes, as well as typical regional scenarios such as conventional plains, high humidity coastal areas, and high-altitude inland areas, the extreme search error is controlled within 0.24%, the recognition accuracy remains above 97.9%, and the warning response time does not exceed 37ms. When t-SNE manifold learning is used for dimensionality reduction, the average projection error is only 2.1%, and after correction, the limit interval error can be controlled within 1%, which is significantly better than PCA method; In the temporary power trading scenario, the algorithm can accurately mark the out of limit interval of the maximum transmission section power exceeding 40MW during the 8.9h-9.1h period. The PMU-based power grid monitoring system accurately issues out-of-limit warnings during this period, and there are no false alarms during other periods, fully verifying the effectiveness of the algorithm in dynamic adaptability, quantitative accuracy, and engineering practicality, providing reliable technical support for the safe and stable operation of the power grid. The application of this algorithm also reflects the development trend of smart grid technology, specifically the utilization of advanced algorithms and monitoring technologies to enhance the intelligence and security of the grid. In the future, with the continuous progress of technology and the continuous optimization of algorithms, it is believed that the security and stability of the power grid will be further improved.

5. Acknowledgement

The study was supported by "Research on Technologies for Enhancing the Safe Operation System of Large Power Grids Based on Intelligent Risk Prevention and Control". (No: 2024-4-72)

References

[1] S. Sepulveda, A. Garcés-Ruiz, and J. Mora-Florez, "Generic optimal power flow for active distribution networks," *Electrical Engineering*, vol. 106, no. 3, pp. 3529–3542, 2024.

[2] X. Su, Y. Ren, and Z. Cai, "A q-learning-based routing approach for energy efficient information transmission in wireless sensor network," *IEEE Transactions on Network and Service Management*, vol. 20, no. 2, pp. 1949–1961, 2023.

[3] A. Lahiru, H. Nasser, G. Ameen, and H. A. Hassan, "Power system reduction techniques for planning and stability studies: A review," *Electric Power Systems Research*, vol. 227, pp. 109917.1–109917.19, 2024.

[4] J. Ling, X. Bian, Y. Yang, L. Xu, M. Zhang, and Z. Liu, "A collaborative planning of pccs siting and transmission network expansion for super large-scale offshore wind clusters," *IET Generation, Transmission & Distribution*, vol. 18, no. 22, pp. 3745–3759, 2024.

[5] P. Kirti, S. Sulabh, G. Fatemeh, and H. Mostafa, "An analysis of the security of multi-area power transmission lines using fuzzy-aco," *Expert Systems with Applications*, vol. 224, pp. 120070.1–120070.11, 2023.

[6] M. Pournabi, M. Mohammadi, S. Afrasiabi, and P. Setoodeh, "Power system transient security assessment based on deep learning considering partial observability," *Electric Power Systems Research*, vol. 205, pp. 107736.1–107736.8, 2022.

[7] P. L. Bhattar, N. M. Pindoriya, A. Sharma, and R. T. Naayagi, "Ac-dc multi-phase power flow algorithms for active distribution system analysis," *Electric Power Systems Research*, vol. 226, pp. 1.1–1.17, 2024.

[8] B. Patel, "Superimposed components of lissajous pattern based feature extraction for classification and localization of transmission line faults," *Electric Power Systems Research*, vol. 215, pp. 109007.1–109007.12, 2023.

[9] M. Shweta, J. Kavita, and C. M. Ramesh, "Appraisal of available transfer capability determination methods in competitive electricity market," *ECS Transactions*, vol. 107, no. 1, pp. 2947–2957, 2022.

[10] P. Sharma, A. Mohapatra, and A. Sharma, "Power circle diagrams and aggregate flexibility curves for active distribution networks," *Electric Power Systems Research*, vol. 206, pp. 107820.1–107820.11, 2022.

[11] J. L. Zhang, S. Liu, and R. Li, "Intelligent perception of operation state of power transmission and transformation equipment based on digital twin technology," *Computer Simulation*, vol. 40, no. 12, pp. 123–127,144, 2023.

[12] Z. Gu, W. Huang, and R. Zhang, "Ultra-large mode area multicore orbital angular momentum transmission fiber designed by neural network and optimization algorithms," *Optoelectronics Letters*, vol. 19, no. 12, pp. 744–751, 2023.

[13] K. Mir and K. N. S. Aalam, "An integrated pmu architecture for power system applications," *International Journal of Emerging Electric Power Systems*, vol. 23, no. 4, pp. 465–495, 2022.

[14] A. Bayat, A. Bagheri, and R. B. Navesi, "A real-time pmu-based optimal operation strategy for active and reactive power sources in smart distribution systems," *Electric Power Systems Research*, vol. 225, pp. 1.1–1.11, 2023.

[15] K. SureshKumar and P. Vimala, "Simultaneous wireless information and power transmission-based power transfer and energy prediction for efficient communication with golden taylor sea lion optimization in wireless sensor network," *International Journal of Communication Systems*, vol. 36, no. 13, pp. e5544.1–e5544.28, 2023.

[16] A. Abdolkhalig, "Innovative method to identify the impedance parameters of a three-phase electric power medium-size transmission line," *Electrical Engineering*, vol. 105, no. 4, pp. 2255–2266, 2023.

[17] R. R. Mohammad, R. H. Seyed, and R. M. Mohammad, "Online identification of power transformer and transmission line parameters using synchronized voltage and current phasors," *Electric Power Systems Research*, vol. 203, pp. 107638.1–107638.10, 2022.

[18] J. Zhao, J. Chen, and Z. Sun, "Channel-feedback-free transmission for downlink fd-ran: A radio map based complex-valued precoding network approach," *China Communications*, vol. 21, no. 4, pp. 10–22, 2024.

[19] M. Kumar and J. Kumar, "Islanding event detection technique based on change in apparent power in microgrid environment," *Electrical Engineering*, vol. 105, no. 3, pp. 1447–1463, 2023.

[20] Y. Zhang, X. Zhang, and X. Ji, "Optimization of integrated energy system considering transmission and distribution network interconnection and energy transmission dynamic characteristics," *International Journal of Electrical Power and Energy Systems*, vol. 153, p. 109357, 2023.

[21] Y. Sang, J. Sheng, and Y. Tian, "Passivity-based sliding mode current control for grid-following modular multilevel converter with system disturbances," *International Journal of Electrical Power and Energy Systems*, vol. 162, p. 110222, 2024.

[22] A. Joshi, R. Khathoon, P. P. V. Devikrishna, and V. V. Angel, "A very fast and easily implementable svm-based relay algorithm to classify the fault and non fault disturbance in vsc hvdc terminals," *Electric Power Systems Research*, vol. 220, pp. 109380.1–109380.11, 2023.

[23] X. Yang and J. Guan, "Pi parameters tuning for frequency tracking control of wireless power transfer system based on improved whale optimization algorithm," *IEEE Access*, vol. 12, pp. 13055–13069, 2024.

Biographies

Ye Zhang holds a Master's degree and graduated from Hunan University. He is a Mid-Level Engineer. He currently works as a Chief Dispatcher in the First Dispatch Department at the Power Dispatch and Control Branch of Inner Mongolia Power (Group) Co., Ltd. His research focuses primarily on power grid dispatch operations and the development and operation of power markets.

Qianpeng Hao holds a Master's degree and graduated from Xi'an Jiaotong University. He is a Senior Engineer. He currently serves as the Director of the Technical Department at the Power Dispatch and Control Branch of Inner Mongolia Power (Group) Co., Ltd. His research focuses primarily on the development of new power grid control systems and power market construction.

Qi Guo is currently pursuing a doctoral degree at Tianjin University and works at the Inner Mongolia Electric Power (Group) Co., Ltd. Electric Power Digital Research Institute, located in Hohhot. As a Professor-level Senior Engineer, his research interests focus on the regulation and control architecture for new-type power systems, power system operation, electricity market construction, digital transformation of power systems, and renewable energy integration.

Shun Yao holds a Master's degree in Electrical Engineering from Hunan University. He currently works at the Electric Power Dispatching and Control Center of Inner Mongolia Power (Group) Co., Ltd. as an intermediate engineer. His main research direction is power system analysis.

Yifan Zhang holds a Master's degree in Electrical Engineering and Automation from the University of Manchester, Automation Supervisor, currently working in Hohhot at the Electric Power Dispatching and Control Center of Inner Mongolia Electric Power (Group) Co., Ltd., Intermediate Engineer. His main research focus is on power grid dispatching and operational management.

Qiang Li holds a Master's degree and graduated from Dalian University of Technology. He is a Senior Engineer. He currently serves as the Deputy Director of the First Dispatch Department at the Power Dispatch and Control Branch of Inner Mongolia Power (Group) Co., Ltd. His research primarily focuses on power grid dispatch operations, power market construction, and renewable energy integration.